CFD INVESTIGATION OF FLUID FLOW AND TURBULENCE FIELD CHARACTERISTICS IN A FOUR-STROKE AUTOMOTIVE DIRECT INJECTION ENGINE

(Date received: 29.1.2007)

Wendy Hardyono Kurniawan, Shahrir Abdullah, Kamaruzzaman Sopian, Zulkifli Mohd. Nopiah and Azhari Shamsudeen

Department of Mechanical and Materials Engineering, Faculty of Engineering
Universiti Kebangsaan Malaysia, 43600 UKM Bangi, Selangor
Email: wendy@eng.ukm.my

ABSTRACT

The CFD simulation to investigate the effect of piston crown inside the combustion chamber of a 4-stroke direct injection automotive engine under the motoring condition is presented. The analyses are dedicated to investigate the outcome of the piston shape differences to the fluid flow and turbulence characteristics for air-fuel mixture preparation in the terms of swirl and tumble ratio, turbulence kinetic energy, turbulence dissipation rate and turbulence viscosity along the degree of crank angle occurred inside this engine. The numerical calculations were performed in a single cylinder of 1.6 litre of a 4-stroke direct injection engine running at wide open throttle condition by using the CFD code to obtain the better piston crown used for such engine. Two different piston bowls for certain engine speeds were considered to be compared to evaluate those mentioned parameters produced during intake and compression stroke. The results obtained from the numerical analysis can be employed to examine the homogeneity of air-fuel mixture configuration for better combustion process and engine performance.

Keywords: *Computational Fluid Dynamics, Combustion, Swirl, Tumble, Turbulence Kinetic Energy, Turbulence Dissipation Rate, Turbulence Viscosity*

1. INTRODUCTION

The engine cycle of typical internal combustion engines consist of four consecutive processes as intake, compression, expansion (including combustion) and exhaust. Of these four processes, the intake and compression stroke is one of the most important processes which influences the pattern of air flow structure coming inside cylinder during intake stroke and generates the condition needed for the fuel injection during the compression stroke. Fluid motion within the engine cylinder is one of the major factors that control the fuel-air mixing and combustion process in spark ignition engines. It also has a significant impact on heat transfer. Both the bulk fluid motion and the turbulence characteristics of the flow are essential to produce the homogeneity structure of air flow come into cylinder. Generally, the initial in-cylinder flow pattern is set up by the intake process and then be substantially modified during compression process. Three common parameters employed to characterise the large-scale mixing in the internal combustion engine are swirl, squish and tumble whereas the small-scale mixing is represented by the turbulence kinetic energy and turbulence kinematic viscosity.

Turbulence inside the cylinder is high during the intake and then decreases as the flow rate slows near the bottom dead centre (BDC). It increases again during the compression stroke as swirl, squish and tumble increase near the top dead centre (TDC). The high turbulence near TDC when ignition occurs is much required for combustion process of the engine. It breaks up and spreads the flame front many times faster than that of a laminar flame. Both fuel and air is consumed in a very short time, whereby self-ignition and knock are avoided. This turbulence is enhanced by the expansion of engine cylinder during the combustion process. The shape of the combustion chamber that is determined by the piston crown plays an important role in maximising turbulence to obtain even mixture of air-fuel composition as well as producing the higher compression ratio.

In turbulent flows, the rates of transfer and mixing are several times greater than the rates due to molecular diffusion. This turbulent diffusion produced from the local fluctuations in the flow field. It leads to increased rates of momentum and heat and mass transfer inside cylinder, which is essential to obtain the appropriate operations of a spark ignition engine. Turbulent flows are always dissipative. Viscous shear stresses execute deformation work on the fluid which will increase its internal energy at the expense of its turbulence kinetic energy so that energy is required to generate turbulence. The character of a turbulent flow also depends on its environment. In the engine cylinder, the flow involves a complicated combination of turbulent shear layers, recirculating regions and boundary layers. The flow is unsteady and may demonstrate the substantial cycle-to-cycle variations. Both large-scale and small-scale turbulent mixing motions are important factors to manage the overall behaviour of the turbulent flow inside engine cylinder.

Recently, besides experiment on the engine test beds, the other advancement for achieving insight into the in-cylinder flow analysis is the application of three-dimensional computational fluid dynamics (CFD) codes. This computer codes are utilised to solve the Navier-Stokes equations to produce detailed descriptions of the mean

velocity and the turbulence velocity fields. While applying to the internal combustion engine case, the CFD models should cover the specific problems related the turbulent flow, high Reynolds number, compressible flow and the complex geometry model. Consequently, the computational time are usually costly and require huge computer memory and even high performance computing (HPC) facilities to save up the work.

Based on the literature studied, there are several researchers have conducted the research on the geometry of a combustion chamber to determine fluid flow using numerical methods. Gosman *et al.* [1] reported the three dimensional of air flow in the engine by utilising the k-ε model, but their research highlighted the phenomenon of the fluid and did not investigate the influence of the involved parameters on the fluid field. Kondoh *et al.* [2] employed a two dimensional axisymmetric turbulent model to study the influence of the combustion chamber shape on the emergence of fluid flow. In addition, Zur Loye *et al.* [3] and Kono *et al.* [4] have performed the calculations of the compression stroke. In particular, Kono *et al.* [4] presented the analysis of the swirl intensity effects on spray formation and obtained reasonable agreement with experimental data. However, since the intake process was not included in the calculation, the initial swirl was imposed as a parameter. It can be mentioned that the way to estimate the initial turbulence between these two studies is different. Because Zur Loye *et al.* [3] obtained it by means of a simplification of the k-ε model, while Kono *et al.* [4] used interpolation from experimental results. Some authors analysed and calculated the intake stroke by introducing some the simplification of their geometry model and its process. Gosman et al. [1] and Wakisaka *et al.* [5] considered the valve as a single moving plate so that the modelling of flow field was very different from the real condition. Moreover, Brandstätter *et al.* [6], Schapertons and Thiele [7] and Theodorakakos and Bergeles [8] have considered the intake valve as a single plate and inflicted the swirl intensity and the intake angle as boundary conditions. Henriot *et al.* [9] made similar simplifications for a spark-ignition engine and obtained reasonably accurate results. Mao *et al.* [10] calculated the intake and compression strokes for an axisymmetric case using a finite element method. In the in-cylinder motion study of Diesel engine, Arcoumanis *et al.* [11] calculated the compression stroke for two different piston bowls, initialising their computation at IVC of induction with a solution obtained previously with simplified flat-topped piston geometry. Aita *et al.* [12] studied the swirl motion in the cylinder during the intake and compression strokes on a real geometry with one intake valve. Chen *et al.* [13] performed calculations of the full intake and compression processes. Dillies *et al.* [14] also presented similar calculations of a Diesel engine with one intake valve for one combustion chamber. Celik *et al.* [15] made a review of computations based on large eddy simulation (LES) and concluded that this method has great potential in this kind of application; however its computational cost is still too high for engine design.

Furthermore, Hyun *et al.* [16] also has performed the numerical simulation by employing the CFD code of KIVA-3 whereby the shape of combustion chamber, swirl intensity, and injection timing are modified and the effect of mixture formation is investigated. The simulation of the detailed in-cylinder air motion during the intake and compression stroke to examine the interaction of air motion with high-pressure fuel spray injected directly into the cylinder also has been accomplished by Kim *et al.* [17]. Lastly, Payri *et al.* [18] who have carried out the CFD modelling of the in-cylinder flow in direct-injection Diesel engines for the intake and compression stroke with different combustion chambers and validate their numerical result with the experimental work.

Therefore, in the present work the CFD code of STAR-CD with the moving mesh and boundary algorithms, including the valves and piston movement capability was carried out to investigate the effect of the piston crown shape to the fluid flow field, turbulence characteristics and the homogeneity of air structure for fuel mixing preparation that occurred inside engine cylinder. The reason is that because the fluid flow with different combustion chamber has an influence in air-fuel mixing, and generation of turbulence as well as exerts great impact on engine performance. Two different combustion chambers with realistic geometry utilised for a compressed natural gas direct injection (CNG-DI) engine will be considered in detail for in-cylinder flow calculations during the intake and compression stroke. The numerical calculation is performed to obtain the optimum conditions mentioned above for the engine model that influence to accomplish the better air-fuel mixing for the rapid combustion process. In order to study the effect of the combustion chamber shape to the fluid flow field for such engine, two characteristics of large scale mixing were analysed in-depth to identify the behaviour of swirl and tumble flow along degree of crank angle. For the purpose of examining the turbulence characteristics occurred within cylinder, three represented parameters from the k-ε turbulence model for high Reynolds numbers exploited was considered in this paper. The three parameters observed, which used to characterise the turbulence intensity field pattern are the turbulence kinetic energy, turbulence dissipation rate and turbulence viscosity. Two mixing parameters, which are very helpful in defining the small scale motion of turbulence, are the turbulence kinematic viscosity and the production of turbulence kinetic energy. Turbulent kinematic viscosity is very significant because it is the primary indicator of spatial locations which are favourable and unfavourable for the survival of large scale coherent structures. The production of turbulence kinetic energy is also useful in capturing the locations where turbulence is being created so that the small scale mixing for the preparation of air-fuel mixture can be enhanced. On the other side, turbulence dissipation rate was employed to define the length scale as the representation of the large scale turbulence.

The computation is numerically calculated and solved the transient analysis of the intake and compression stroke for the piston crown under engine speed at 2000 rpm and equipped its boundary condition. The five parameters for the fluid flow and turbulence characteristics acquired from the simulation will be taken into account to verify the homogeneity of air structure for mixture preparation so that the better air-fuel mixture and combustion process can be achieved. In this work, no simplifications of the geometry model were constructed and the intake calculations involve the intake port and moving valves so that the flow field could be analysed completely. In particular, the differences observed for the two different piston bowl shapes in the parameters configuration of fluid flow and turbulence characteristics during the intake and compression stroke are discussed and some conclusions can be drawn out. In general, this study provides an insight of the influence of the piston bowl shape on the characteristics of air structure pattern for a direct injection engine.

2. CFD STRATEGY OF ENGINE MODELLING

The CFD simulations presented in this paper were carried out for the intake and compression strokes using the algorithm of mesh and boundary movements [19]. The moving mesh was treated by applying the Arbitrary Lagrangian-Eulerian (ALE) for

the typical events occurred in the internal combustion engine, including the valve and piston movement. Every contained event represents the different mesh and boundary geometries for every different crank angle in each step of engine cycle. Hence, in order to perform the proper CFD simulations for the internal combustion process, the analysis and calculation should be carried out using the unsteady (transient) calculation, moving meshes and boundaries, high compressible Reynolds number, high fluid dynamics characteristics (turbulence intensity), momentum, heat and mass transfer and complex geometries model and chemical-thermal dependent as well.

The equations employed to describe mass, momentum, energy and k-ε turbulence model in the vector notation without source terms from spray and chemical reactions due to under motoring condition are expressed as follows:

$$\frac{\partial \rho}{\partial t} + \nabla \cdot \left[\rho \vec{u} \right] = 0 \tag{1}$$

$$\frac{\partial \rho}{\partial t} \left[\rho \vec{u} \right] + \nabla \cdot \left[\rho \vec{u} \vec{u} \right] = \nabla P - \nabla \left[\frac{2}{3} \rho k \right] + \nabla \cdot \vec{\sigma} + \rho g \tag{2}$$

$$\frac{\partial \rho}{\partial t} \left[\rho I \right] + \nabla \cdot \left[\rho I \vec{u} \right] = P \nabla \cdot \vec{u} - \nabla + \nabla \cdot \vec{J} + \rho \varepsilon \tag{3}$$

$$\frac{\partial}{\partial t} (\rho k) + \nabla \cdot \left[\rho \vec{u} k \right] = -\frac{2}{3} pk \nabla \cdot \vec{u} + \vec{\sigma} \cdot \nabla \vec{u} + \nabla \left[\left[\frac{\mu_t}{\mathrm{Pr}_k} \right] \nabla k \right] - \rho \varepsilon \tag{4}$$

$$\frac{\partial}{\partial t} (\rho \varepsilon) + \nabla \cdot \left[\rho \vec{u} \varepsilon \right] = - \left[\frac{2}{3} c_{\varepsilon 1} - c_{\varepsilon 3} \right] \rho \varepsilon \nabla \cdot \vec{u} + \nabla \cdot \left[\left[\frac{\mu_t}{\mathrm{Pr}_\varepsilon} \right] \nabla \varepsilon \right] +$$

$$\frac{\varepsilon}{k} \left[c_{\varepsilon 1} \vec{\sigma} : \nabla \vec{u} - c_{\varepsilon 2} \rho \varepsilon \right] \tag{5}$$

where ρ is the density; $\vec{u}$ the velocity vector; P the pressure; $\vec{\sigma}$ the turbulent viscous stress tensor; I the specific internal energy and $\vec{J}$ the heat flux vector including turbulent heat conduction and enthalpy diffusion effects. The turbulence viscosity term is described as below:

$$\mu_t = c_{\mu\rho} \left[\frac{k^2}{\varepsilon} \right] \tag{6}$$

Those constants in Equations (4), (5) and (6) are given as:

$c_{\varepsilon 1} = 1.44$; $c_{\varepsilon 2} = 1.92$; $c_{\varepsilon 3} = -1.0$; $\mathrm{Pr}_k = 1.0$; $\mathrm{Pr}_\varepsilon = 1.3$ and $c_\mu = 0.09$

The computed turbulence dissipation length scale is obtained from the k-ε results as:

$$L_\varepsilon = c_\mu^{3/4} \frac{k^{3/2}}{k \cdot \varepsilon} \tag{7}$$

where ϰ is the Von Karman constant. The accompanying result of the k-ε model is the turbulence intensity which is assumed as:

$$u' = \sqrt{\frac{2k}{3}} \tag{8}$$

3. DESCRIPTION OF ENGINE GEOMETRY AND CONDITIONS

The engine model studied is a typical single-cylinder of a CNG-DI engine with two intake and exhaust valves as shown in Figure 1 and equipped with two considered pistons shapes as depicted in Figure 2. As mentioned, two piston crowns were considered to investigate the behaviour and pattern of swirl, tumble and turbulence intensity field occurred inside cylinder in order to obtain the suitable piston shape for the combustion process of such engine. These two shapes are representative of the real engine geometry model that usually operated to obtain the higher compression ratio as well as the optimum combustion process in a CNG-DI engine. Piston A has a bowl at the centre of its crown while piston B has the deeper bowl volume than piston A and not located in the centre.

Figure 1: A schematic view of typical engine model with piston crown A

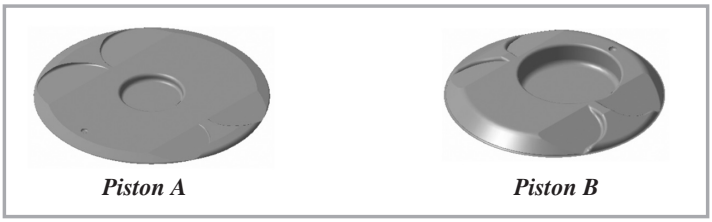

Figure 2: Geometry of the combustion chamber

The specifications and characteristics of the operating condition from the engine model studied that will be employed for the computational and boundary condition of CFD analysis during the intake and compression stroke is summarised by Table 1. The engine is a typical four-stroke automotive engine with direct injection system. The fuel injector is located centrally inside the combustion chamber and spark plug is positioned at the vicinity area of it to provide the homogeneous mixture and rapid combustion process.

4. MESH GENERATION

A grid generation program has been exploited to generate the grid to create the hexahedral cells for the engine model. The computational domain for the CFD calculation covers the intake ports and valves, the cylinder head and the piston bowl as shown in Figure 3(a). The number of cells varies from 90,000 cells in TDC and around 180,000-200,000 cells in BDC, where about the half of the cells used to generate the mesh at the cylinder head and piston bowl in the case of considering the grid sensitivity and reasonable

Table 1: Specification of the engine model for computational condition

Engine Parameters	Value
Number of cylinders	4
Type	Inline
Displacement Volume	1596
Bore	78
Stroke	84
Connecting rod length	131
Crank radius	44
Compression ratio	14
Intake valve opening	12
Intake valve closing	48
Exhaust valve opening	45
Exhaust valve closing	10
Maximum intake valve lift	8.1
Maximum exhaust valve lift	7.5
Combustion chamber	Bowl piston

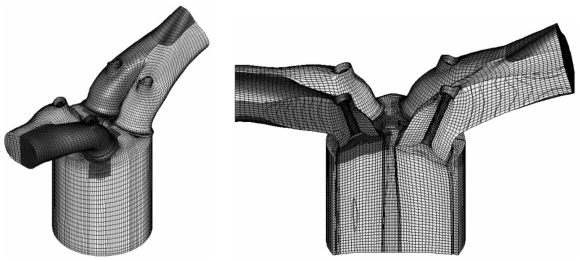

(a) *(b)*

Figure 3: The computational domain of the engine model and its clipped section view

computer run time. The fine grid structure is necessary for mesh snapping during the valve movement. The hexahedral cells have been adopted for the mesh generation because they provide a better accuracy and stability compared to the tetrahedral cells. The much important motivation about the use of hexahedral cells is the requirements of moving meshes and boundaries to accomplish the CFD calculation.

Because of complexity of the engine model, the computational mesh is divided into four areas with different topologies, where each area has been meshed separately as also shown in Figure 3(b). This approach is used to obtain a good quality grid (mesh) and to reduce the meshing time significantly. The connectivity of the various sub-domains is ensured by means of arbitrary interfaces that connect every faces of the zones. Both intake ports meshes have been created using a similar topology, where the cell are oriented in the flow direction and joined with a cylindrical structured mesh in the zone upstream of the valves. The grid above the valves both intake and exhaust has been constructed by the revolution of a structure mesh section. During the compression stroke, when the intake valves are closed, the sub-domains of intake ports are already disconnected from the calculation to reduce the computational time and cost as well. As the total number of computational cell is around 180,000-200,000 cells, the typical CPU time taken for the simulation of complete intake and compression stroke with the fluctuate time steps is around 10 hours on a 4 CPU-SGI Origin 300 with 56 MB dynamic memory used during the running analysis.

5. NUMERICAL METHODOLOGY

The CFD code of STAR-CD for finite volume method has been utilised to solve the discretised continuity and Navier-Stokes equations. This CFD code is commonly used for the internal combustion engine and has the high capability of solving the transient, compressible, turbulent-reacting flows with sprays on the finite volume grids with moving boundaries and meshes. Fully hexahedral meshes of intake and exhaust ports and combustion chamber are utilised here due to the requirements of moving mesh. Piston and valve motion are carried out by cell activation and deactivation, and supported by vertex motion routines. The code is competent of handling the complex geometry and enabling the computational domain to include the intake and exhaust ports, valves, valve seats and the combustion chamber with moving piston.

The numerical methodology and computation of the present internal combustion engine study is based on the pressure-correction method and the pressure implicit splitting operator (PISO) algorithm. The second upwind differencing scheme (MARS) as the spatial discretisation is used for the momentum, energy and turbulence equations. The temporal discretisation is the implicit method, with variable time step depending on the stage of the engine cycle. At the beginning and the end of the intake stroke, when the valve lift is quite small, there are high local velocities in the discharge zone. Therefore, the time step must be small enough as 0.1 CAD per iteration in order to accomplish the stability criterion [20]. During the middle phase of the intake stroke and also during the compression stroke, before the piston reaches TDC, the time step is set up at the 0.25 CAD per iteration by reason of the highly computational cost since there are no high local velocities and the effect of the squish and tumble during compression stroke does not so much effect to the calculation. Finally, near TDC, the time step must be reduced again to 0.1 CAD per iteration because of the effect to tumble and the small clearance between the piston and the cylinder head.

The running calculations started when intake valve opening and continued to the compression stroke without the fuel injection. These both variables are calculated as homogeneous in the whole domain. The valve overlap period is also taken into account when the residual gases come out from the exhaust port. The initial values for pressure and temperature for engine operating speed of 2000 rpm were obtained from the experimental work and test from a single cylinder research engine test bed. The initial turbulence intensity was set at 3% of the mean flow, which is quite sufficient for fully turbulent fluid flow, whereas the integral length scale was specified proportional at 0.4% based on the Prandtl's work as a result of the distance to the nearest solid wall [21]. Constant pressure boundary conditions were carried out at both intake and exhaust ports so that the dynamics effects were neglected. The walls of the intake and exhaust ports and the lateral walls of the valves were considered as the adiabatic condition. The constant temperature boundary conditions were allocated independently for the cylinder head, the cylinder wall, and the piston crown that outline the walls of the combustion chamber. The temperature on each of these walls will be calculated numerically in the form of iteration for every time step automatically.

6. RESULTS AND DISCUSSIONS

The detailed numerical study to investigate the effect of the piston crown shape to the fluid flow field and turbulence characteristics for a 4-stroke direct injection engine under motoring condition has been carried out. The results presented are divided into two important sections for fluid flow field and turbulence characteristics, which are completed with its discussions for the two different piston shapes. In addition, the graphs of global variations for each considered parameters are plotted according to degree of crank angle.

6.1 FLUID FLOW FIELD

In this section, the velocity vector field as the large-scale mixing during the intake and compression stroke in the cylinder for two piston crown will be analysed and investigated. To analyse in-cylinder air motion inside the cylinder, swirl and tumble ratios for both on the sideways and normal directions are calculated at each time step or every crank angle degrees of engine cycle to identify the behaviour of fluid flow field characteristics among two different piston shapes.

As mentioned previously, swirl and tumble flows are always generated during intake and compression stroke of the internal combustion engine due to the high turbulence in the cylinder. Swirl refers to a rotational flow within the cylinder about its axis and is used to promote rapid combustion. And tumble is a rotational motion about a circumferential axis near the edge of the clearance volume in the piston crown or in the cylinder head, which is caused by squishing of the in-cylinder volume as piston reaches near TDC. Both swirl and tumble flows are commonly characterised by a dimensionless parameter employed to quantify rotational and angular motion inside the cylinder, which are known as swirl and tumble ratios, respectively. These values are calculated by the effective angular speed of in-cylinder air motion divided by the engine speed. The effective angular speed is the ratio of the angular momentum to the angular inertia of moment. The mass centre of the charged in-cylinder air is considered as an origin for the calculation.

The three variables (swirl, sideways tumble, and normal tumble ratio) investigated in this paper are presented in the non-dimensional form by applying the equations as follows:

$$SR = \frac{60H_z}{2\pi I_z \omega} \tag{9}$$

$$TR_x = \frac{60H_x}{2\pi I_x \omega} \tag{10}$$

$$TR_y = \frac{60H_y}{2\pi I_y \omega} \tag{11}$$

where H_x, H_y and H_z is the angular momentum of the in-cylinder gas about the *x* axis, *y* axis and *z* axis, respectively. I_x, I_y and I_z is the moment of inertia about the x axis, y axis and z axis, respectively. In addition, ω is the crankshaft rotation or engine speed in the unit of rotation/minute.

A schematic view of reference axes for the analysis and calculation is presented in Figure 4. The origin of the coordinate systems shown in the figure is only for a reference to illustrate swirl and tumble directions and magnitudes. The in-cylinder air motion before fuel injection process is such important to certify a proper air-fuel mixture, which finally affects on the complete combustion in the engine cylinder. In the following some details of in-cylinder air motion without fuel injection during intake and compression stroke for are figured out to verify the velocity vector and turbulence intensity fields in the form of swirl and tumble flow and turbulence kinetic energy, respectively.

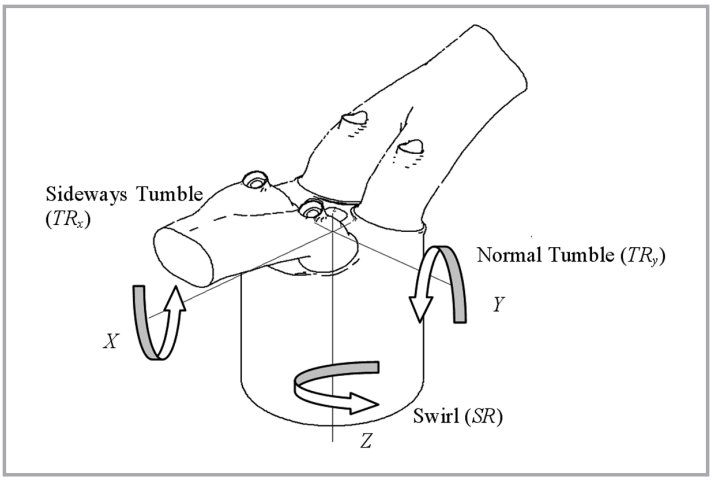

Figure 4: Schematic view for the definition of swirl and tumble axes and directions (SR: swirl ratio, TRx: sideways tumble ratio, TRy: normal tumble ratio)

Figure 5 shows the velocity fields during the intake stroke (100º after TDC) for two combustion chambers on the XY cutting plane (at Z = 10 mm of cylinder head axis) as shown in the top figure, the XZ cutting plane (at Y = 7 mm) as shown in the middle figure and the YZ cutting plane as shown in the bottom figure. It can be seen that there are strong annular jet flows for two combustion chambers in the area near the valve curtains because the flow and velocity field in this degree of crank angle reaches to the maximum value where the intake valves almost open at the maximum lift distance. And this strong annular jet flows make a clockwise swirl on the one intake valve and a counter-clockwise on another intake valve as shown clearly for each piston crown shape. At this stage, the piston speed is nearly constant and the intake valves are almost fully open (maximum lift). The toroidal vortex that developed in the early part of the intake stroke has already disappeared. Nevertheless, a new clockwise vortex can be seen in the centre of the engine cylinder, especially under intake valves as a result of the jet motion towards the central part of the cylinder, which does not collide directly with the cylinder walls. This annular jet flows that impinges on the wall is deflected axially towards the piston with centre bowl and produces an elongated vortex along the wall. In addition, the top figure confirms that there are several vortices exist with no predominant pattern and there is symmetry flow field due to a vertical plane situated between the two intake valves.

During the later phase of the compression stroke, the axial upwards field encourages a gradual increase of the swirl velocity in the top part of the piston crown as shown in Figure 6 for two piston crowns. It also can be pointed out that when the piston at the position of 30º before TDC, the axial velocity vector of air in the engine cylinder is practically complete to be mixed with the fuel in many areas or zones. During the compression stroke, the turbulence generated by the annular jet flows during the previous intake stroke decay quite quickly and remains seem to be distributed homogeneously along the engine cylinder. The combustion chamber shape of an internal combustion engine is basically does not alter the global in-cylinder air motion but it is

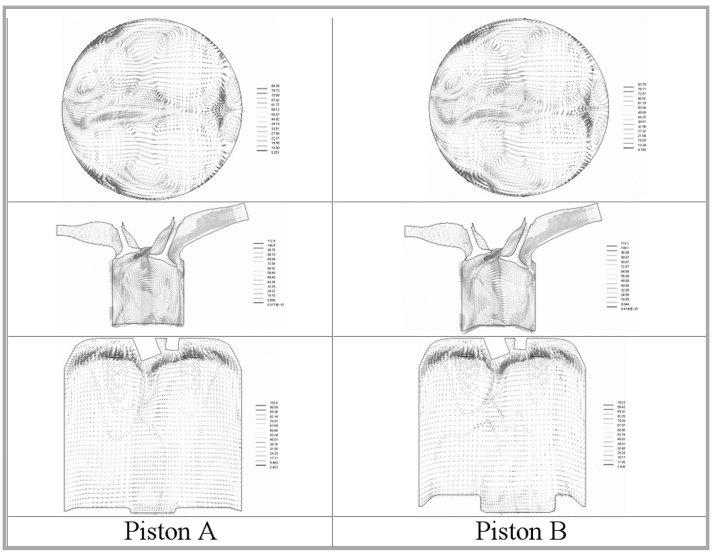

Figure 5: Velocity vector field during intake stroke (100º after TDC) on the XY plane (top), the XZ plane (medium) and the YZ plane (bottom)

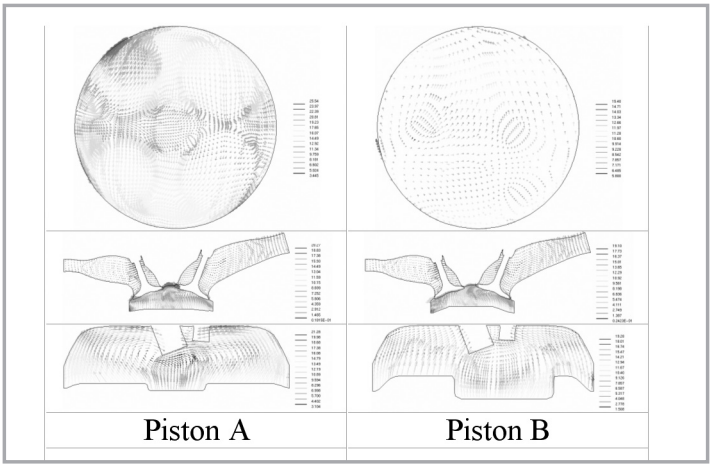

Figure 6: Velocity vector field during compression stroke (30º before TDC) on the XY plane (top), the XZ plane (medium) and the YZ plane (bottom)

affect to the velocity field close to the piston top surface (near cylinder head) during the later phase of compression stroke where the fuel injection start to begin and the spark plug is ready to burn the air-fuel mixture to start off the combustion process. One important thing to be noticed in the in-cylinder analysis of the engine is that the composition of air mixture is homogeneous enough before the fuel is injected directly into the bowl of piston and ignited by spark plug to start the combustion process.

The global variations of swirl ratio for the two pistons are calculated and displayed in Figure 7. For the purpose of computing swirl ratio, the reference values for x and y are taken at the cylinder axis where x = 0 and y = 0. As can be seen from the graph, the swirl in the cylinder is generated early during the intake stroke. The maximum is achieved near around 140º after TDC, where the piston reaches its maximum instantaneous speed and the valve opening is in its maximum distance. After that, the discharge velocity into the cylinder decreases and swirl will decline slowly during the rest of the intake stroke. In the first part of the compression stroke, the trend continues to decrease due to the friction at the cylinder wall. However, swirl is developed as the flow accelerates in preserving its angular momentum within the smaller diameter piston bowl when approaching TDC. During the compression stroke, swirl is necessary needed to interact with squish flow to generate a very complex flow field for the purpose of enhancing air-fuel mixture during fuel injection. In fact, piston A is able to generate higher swirl ratio than piston B with small range differences during intake and compression stroke. From the analysis, it can be verified that the capability of producing swirl ratio for two different combustion chambers at same engine speed is relatively different due to the friction within cylinder wall and its intake air flows influenced by combustion chamber head.

Subsequently, the behaviour and variation of tumble flow in the sideways direction inside engine cylinder can be seen in Figure 8. Tumble about the x-axis becomes negative in the early of the intake stroke and reaches a minimum at around 60º after TDC. After this crank angle, there is a quick change, which leads to a maximum positive tumble at around 150º after TDC. This difference condition can be attributed to the development of the two dominant vortices caused by the jet-bulk flow interaction. As the valve lift near to the closed position, the tumble ratio at the x-axis will be decreased gradually until the early part of the compression stroke before going up again during the middle of the compression stroke. After that, the sideways tumble ratio will decrease at the certain degree of crank angle near TDC. The extraordinary thing to be mentioned here is that the piston B produces the much lower magnitude of sideways tumble ratio along the rest part of the compression stroke. This condition means that the piston B is not able to produce the homogeneity of air structure along cylinder, which needed to prepare the condition for fuel injection period.

The investigation of tumble ratio in the normal direction finally can be figured out in Figure 9. The figures show the normal tumble ratio and its variation occurred inside engine cylinder. Tumble

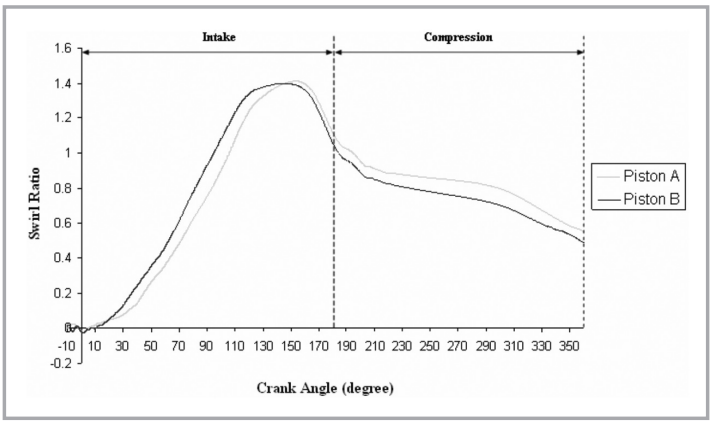

Figure 7: Calculated swirl ratio versus crank angle

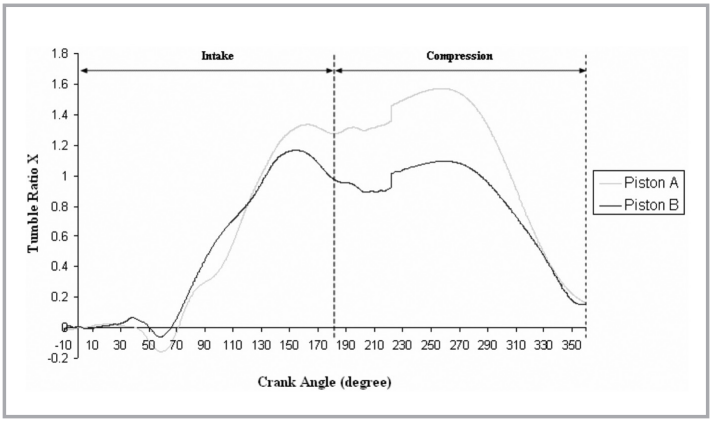

Figure 8: Calculated sideways tumble ratio versus crank angle

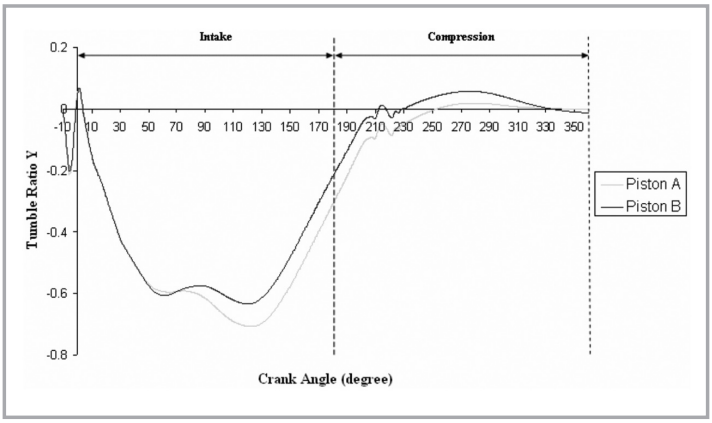

Figure 9: Calculated normal tumble ratio versus crank angle

about the y-axis begins with a negative sense and changes its sign dramatically at the early part of intake stroke. This transient behaviour is characterised to the very complex nature of the early flow field. By 120º after TDC, a dominant tumbling motion has been developed and decreased incrementally as the valve lift closes until the early part of the compression stroke. And then, it will increase again slightly at the middle part of the compression stroke before diminishing again as piston approach TDC. From Figure 9, it can be concluded that piston A can generate higher tumble ratio on the normal side (y-axis) during early intake stroke. This circumstance means that the shape of piston A plays an important role in producing the fluid dynamics parameters during intake and compression stroke as it has been determined from CFD analysis that piston A has the capability of producing better fluid flow field characteristics.

6.2 TURBULENCE FIELD

From the viewpoint of the fundamental turbulence physics, the major two parameters required to characterise the turbulent flow characteristics are the turbulence kinetic energy (k) and its dissipation rate (ε). The turbulence kinetic energy is related to the turbulence intensity, which is a measure of the characteristics speed of the turbulent flow over a distance characteristic. On the other side, the turbulence dissipation rate is associated to the turbulence length scale, which is a quantitative measure of the distance characteristics of the flow structure. An important small scale mixing parameter which is a combination of turbulence kinetic energy (k) and its dissipation rate (ε) is referred to as the turbulence kinematic viscosity.

The production of turbulence kinetic energy is very insightful in characterising the in-cylinder locations where turbulence is being created. The significance of production term is that it elucidates the contributions of both the in-cylinder velocity fields and the turbulent kinematic viscosity in order to produce the turbulence kinetic energy. Generally, without in-cylinder velocity fields, the turbulence will not be generated and the current level of in-cylinder turbulence will continuously deteriorate until its energy has entirely dissipated along the chamber walls. Specifically, in-cylinder turbulence can be beneficial for gaining the optimum air–fuel mixing preparation before fuel injection and increasing combustion rates.

The turbulence kinetic energy during intake stroke can be found out from the XZ cutting plane to verify the generation of air structure inside cylinder (Figure 10). The turbulence intensity field is presented in the form of isoline contours due to its clear appearance. It appears clearly distributed uniformly for piston A and B, where the large values occurred in the area near the top region the cylinder, especially around the valves and close to the cylinder wall where there is a jet impingement. The other important thing to be mentioned is that the level of turbulence kinetic energy is relatively low in the bottom part of the cylinder and in the piston bowl.

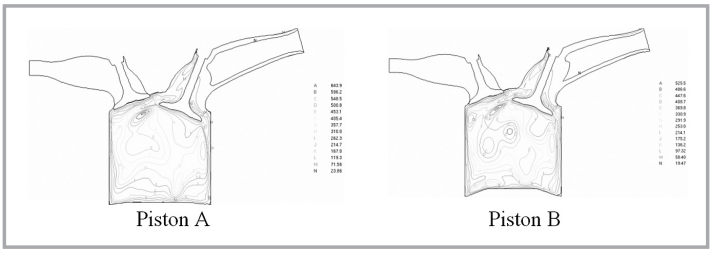

Figure 10: Turbulence kinetic energy during intake stroke (100º after TDC)

The turbulence intensity field in the form of the turbulence kinetic energy during the compression stroke, which near TDC will be discussed and the result is displayed in Figure 11. As can be seen, the isoline contours from two pistons are quite different, where piston B has the highest value of turbulence field and piston A has the lowest one. It is important to note here that the behaviour of air flow before fuel injection among two pistons shows the dissimilar homogeneity. This means that the combustion chamber inside cylinder does play a major role in the turbulence generation during the compression stroke. The maximum value for piston A is observed on the exhaust side of the chambers. On the other hand, the maximum value for piston B is almost disappeared and also occurs at the bottom of exhaust side of chambers. From this numerical prediction of air structure, it can be concluded that the homogeneity of air structure needed before the fuel injection and spark ignition process is tend to be occurred in piston A due to the reason of the value of turbulence kinetic energy produced during the compression stroke. The other important thing to be considered is that its maximum value arises in the zone near the hole injector so that the air will contain the homogeneous condition before the fuel is injected directly into the chamber.

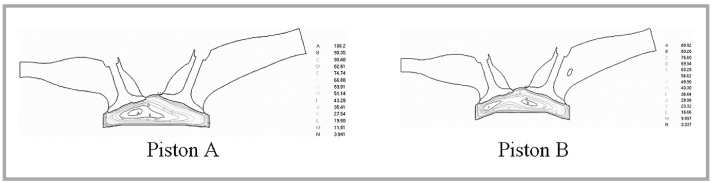

Figure 11: Turbulence kinetic energy during compression stroke (30º before TDC)

The generation of turbulence kinetic energy during the intake and compression stroke can be defined as the turbulence intensity (m/s) from the k-ε model obtained by using the Equation (8). The turbulence intensity for two pistons during the intake and compression stroke can be plotted in Figure12. During the early stages of the intake stroke, the jet flow interactions are the most important mechanism for the production of turbulence intensity. The early fluctuation of turbulence intensity is due to the sudden opening of intake valve and closing of exhaust valve. Before 40º after TDC, the turbulence intensity increases rapidly and reaches its maximum value in the quarter part of intake stroke. At the maximum valve lift, the production associated with the jet interaction penetrates to the middle of engine cylinder and the production related to the jet-bulk flow remains very homogeneous or stratified along the cylinder

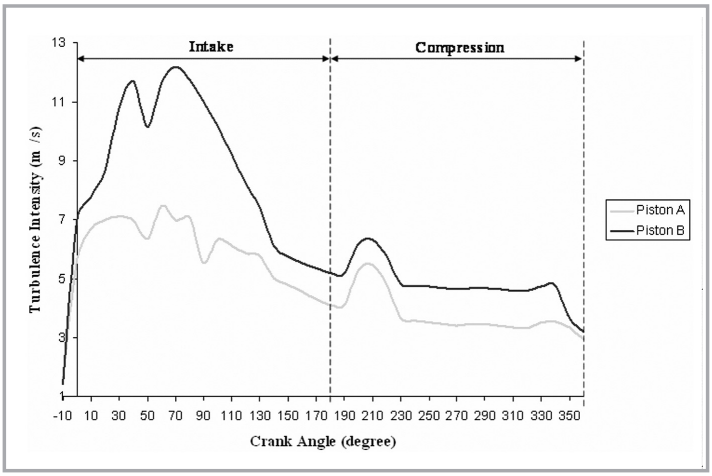

Figure 12: Calculated turbulence intensity versus crank angle

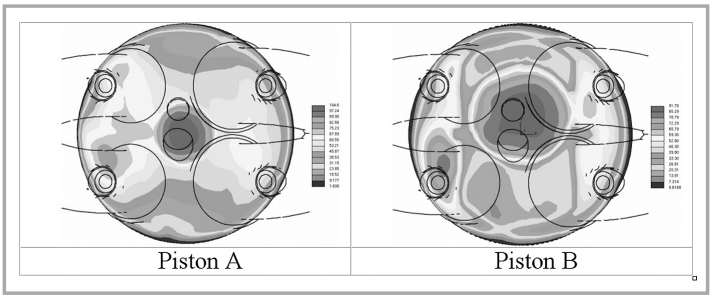

Figure 13: Turbulence kinetic energy on 10 mm below the cylinder head at 20º before TDC

head. This behaviour continues throughout the intake stroke. Upon valve closure, the intake jets are no longer exist and the velocity gradients associated with them will disappear. This condition will lead to an overall decrease in the production of turbulence near the cylinder head because of the absence of an active mechanism for generating the turbulence kinetic energy. However, as the piston moves upward during the compression stroke, the production of the turbulence kinetic energy is investigated along the rim of the piston bowl on the upwind side of the cylinder and along the cylinder head caused by the recess in the head for the upwind valve. As can be seen, piston B has the capability of producing the higher turbulence intensity compared to piston A due to its piston shape which has more in-depth bowl. During intake stroke, piston B has higher turbulence intensity which exceed up to 12 m/s while piston A only has the value of 7 m/s. However, the higher turbulence intensity produced by piston B decreases during compression and approach the magnitude generated by piston A. In the last part of compression, the turbulence intensity from piston A and B approach the same value.

The locations where turbulence kinetic energy produced are useful in order to distinguish the small scale mixing for the preparation of spark ignition for the rapid combustion process. The turbulence kinetic energy produced at the 20º before TDC for the preparation of spark ignition timing for two different shape of combustion chamber can be presented in Figure13. As can be seen, the highest turbulence kinetic energy is produced by piston A where its condition is more homogeneous along cylinder head that can be utilised importantly to prepare the flow field structure before ignition timing for the combustion process later. The actual condition for piston B is that it has the capability to produce the higher turbulence kinetic energy on the region around the spark plug location, but its value is not as high as that of piston A.

The production and destruction of turbulence kinetic energy are always closely associated with the turbulence dissipation rate. The dissipation rate ε is large where production of *k* is large. As cited previously, the turbulence dissipation rate is related to the turbulence length scale, which is a quantitative measure of the distance characteristics of the flow structure. The appearance of turbulence dissipation is quite obliging in locating the shearing rates occurs within cylinder which is a disadvantage for engine performance.

The turbulence dissipation rate during intake stroke can be observed in Figure 14 in three-dimensional view to capture the generation of shear rate within cylinder. The turbulence dissipation rate here is displayed in the appearance of contour plot to identify the locations of shearing stress. It appears clearly for piston A and B that the shear rates take place in the area near the top region of the cylinder due to its valves recess position especially around the valves seat where there is a strong jet impingement. The same condition is also occurred during the compression stroke as can be depicted in Figure15 showing the red contour plot exists in the region of valve seat causing the large shearing rate happened in such region.

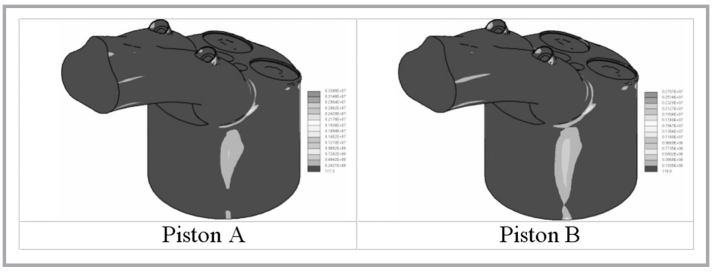

Figure 14: Turbulence dissipation rate during intake stroke (100º after TDC)

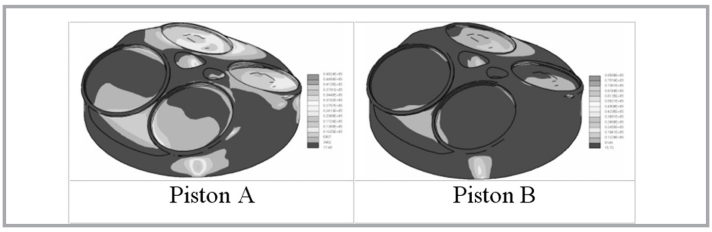

Figure 15: Turbulence dissipation rate during compression stroke (30º before TDC)

The plotted graphs to show the behaviour of turbulence dissipation rate are shown in Figure 16 versus crank angle degree during the intake and compression stroke. It is defined as the turbulence length scale (mm) from the k-ε model employed and obtained by utilising Equation (7). Early in the intake stroke, as the piston velocity increases rapidly and the valve lift distances are still small, the fluid velocities at the region of the curtain area become very large. These large intake velocities lead to high shearing rates because of the dynamic interactions between jets with jets, jets with walls and jets with bulk flows, which tend to enhance the turbulence dissipation rate. As the valve lift increases around 80º after TDC, the level of turbulence length scale begin to decrease due to the larger curtain areas which lead to lower shearing rates resulting from lower velocities. The fluctuations in turbulence length scale continue until late in the intake stroke as the valve lift becomes small again. Then, an increment in turbulence length scale was observed, which is caused by the heightened shear along the curtain area because of the minimal valve lifts. This behaviour proceeds until the time of intake valve closing. Upon intake valve closure, the

turbulence length scale enlarges continuously until the squish flow is exhibited near TDC. This behaviour is consistent with the decay of large scale structures throughout the compression stroke which has been discussed previously in this work. As shown in Figure 16, the turbulence length scale of piston B is relatively higher than that of piston B during intake stroke. However, during compression stroke, the turbulence length scale of piston A reaches the value of around 2.5 mm compared to the value produced by piston B. These phenomenons are occurred due to the effect of piston shape, which cause the fluctuations of turbulence parameters.

The observations carried out on the combination of turbulence intensity and length scale show that the strong intake jet produces small eddies with high turbulence intensity during intake stroke. The turbulent kinetic energy decreases but the turbulence dissipation rate increases at the end of intake stroke. The tendency from the present numerical study indicates that the energy which contains eddies increase in size but decrease in strength during intake period. Both turbulence intensity and length scales decrease to certain value near TDC during the closed period. This is happened due to the compression effect of the moving piston.

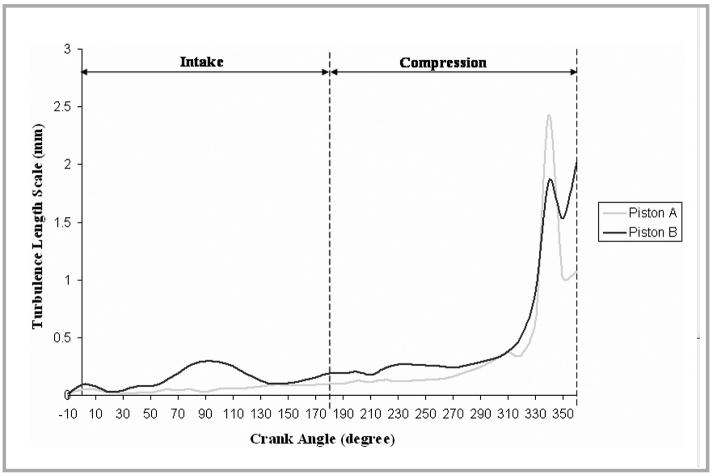

Figure 16: Calculated turbulence length scale versus crank angle

The enhanced small scale mixing inside engine cylinder can be quantified through turbulence kinematic viscosity. The turbulence kinematic viscosity is an insightful tool for mixing parameter because of its effects on large scale structures. Regions of heightened in-cylinder turbulence kinematic were observed to be highly dissipative of large scale structures. Therefore, the turbulence kinematic viscosity is an important indicator to detect the spatial locations where there large scale coherent structures can be survived favourable and unfavourable. Figure17 shows the cutting view of middle cylinder for the computed turbulence kinematic viscosity during intake and compression stroke, respectively for two piston crowns. As can be seen, it represents the structure of small scale mixing within cylinder to be examined for obtaining the better mixing preparation for fuel injection process. In this figure, the small structure of scale motion during intake stroke occurs in the region under intake valves due to its downward motion. This motion has an influence on the character of the intake jets, which causing the decreased production of turbulence kinetic energy and increased turbulence dissipation rate. In the period of intake stroke, the turbulence kinematic viscosity generated by piston A is larger compared to the turbulence kinematic viscosity produced by piston B. The phenomenon concluded from such physical condition is that piston A creates weak intake jet for low turbulence intensity with larger dissipation rate due to its shape of piston crown. During the closed period, the small scale motion generated before TDC can be presented in Figure 18. As can be noticed, the scale motion is produced in the middle of engine cylinder symmetrically and need to be taken into account for air-fuel mixture process before spark ignition begins. The magnitude of turbulence kinematic viscosity produced by piston B when compressing upward to TDC is quite higher compared to piston A because piston B has the ability to generate higher turbulence intensity with lower dissipation rate due to its complex piston shape with deep bowl. The turbulence kinematic viscosity shown here proves that the its generation is much depend on the piston crown due to its compression capability up to the head of combustion chamber.

The global variations of turbulence viscosity, which represents the small scale mixing during intake and compression stroke, can be plotted in Figure 19 and it is calculated using the Equation (6). Its values begin low at the early time of intake valve opening before maintaining its constant value during the later part of intake stroke. During intake valve closure, its value starts to ascend the maximum value at the crank angle position near TDC because of the compression effect of the piston motion when squeezing the air upward. Afterwards, the value will decline a little bit to become weak before the piston touches TDC. The physical condition can be understood from this phenomena is that the spark ignition timing to initiate the flame propagation for the start of combustion process usually should be done at the crank angle around 10º-20º before TDC when the magnitude of turbulence kinematic viscosity is still relatively high. It can figured out that the magnitude of turbulence kinematic viscosity from piston A reaches the value of around 0.02 Pas and it is higher than the value of piston B. Unfortunately, the behaviour is changing during compression stroke, in which piston produces the higher turbulence kinematic viscosity due to its more in-depth bowl shape.

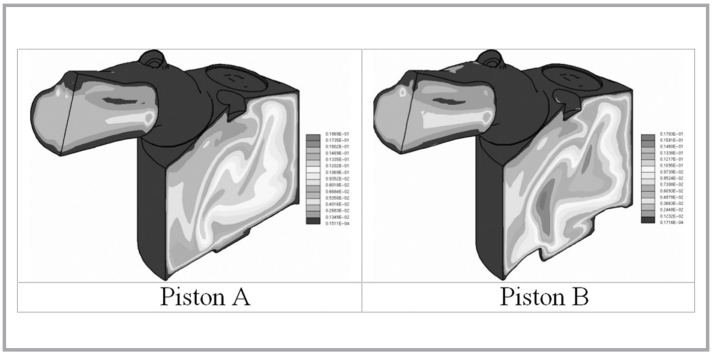

Figure 17: Turbulence kinematic viscosity during intake stroke (100º after TDC)

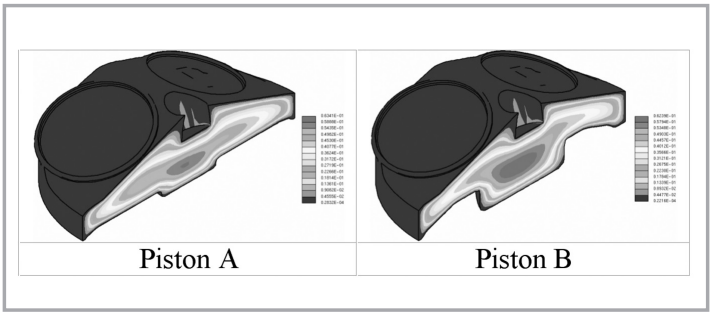

Figure 18: Turbulence kinematic viscosity during compression stroke (30º before TDC)

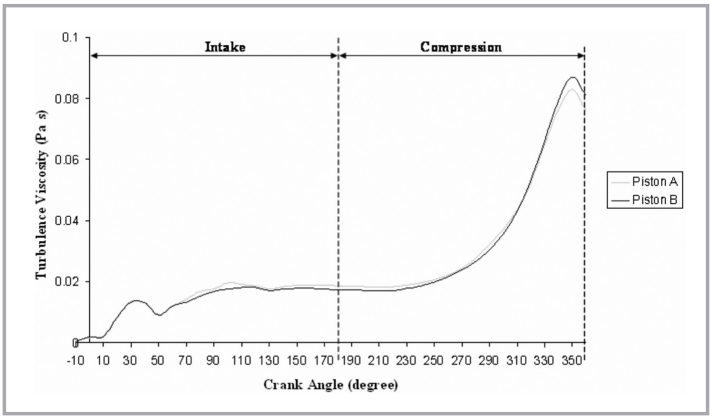

Figure 19: Calculated turbulence kinematic viscosity versus crank angle

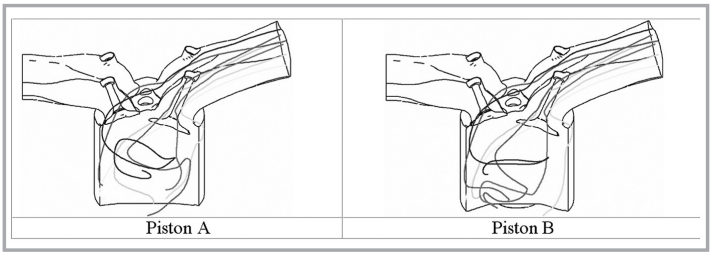

Figure 20: The computed streamlines at 108º aTDC (intake stroke) showing the swirl and tumble structure as large scale motion

Lastly, the other in-cylinder feature characteristic to examine the air flow inside cylinder and perceive the effect of combustion chamber shape is the unsymmetrical structure of the flow (Figure 20). In this figure, the instantaneous streamlines at 108º after TDC, represented by continues lines, are shown. There are some streamlines presented to simulate the air-flow motion inside combustion chamber as it can be seen that the swirl is already generated at some location of cylinder wall during intake stroke. As indicated by the symmetrical projections of the streamlines, the flows are seen to be quite symmetrical about the centre plane between two valves due to the symmetrical runner, port and valve setting. This symmetrical flow structure and pattern implies that the bulk flows from the two valve openings do not mix together significantly. As can be seen, the blue line of piston A streams cylindrically inside cylinder when the air comes in from intake port at the maximum valve lift if comparing to the air mixture of piston B. This condition will give a clear phenomenon that the piston A can be adopted to give a homogeneous condition, which proved by the CFD calculation instead of experimental test. It is interesting to notice that the investigation of air motion (swirls and tumbles behaviour) in the combustion chamber can be carried out by using the CFD code.

7. NUMERICAL VALIDATION

The experimental setup for the purpose of validating the CFD simulation was carried out in a test rig of single cylinder research engine (SCRE) as shown in Figure 21. The available data used for the numerical validation was performed by considering some important technical aspects. During the experiment, all engine boundary conditions were fixed. Piezoelectric pressure sensors (Kistler 6061B) were installed on the combustion chamber to measure the cylinder pressure occurred during combustion process. In order to obtain the boundary conditions at the intake and outflow boundaries for the CFD analysis, thermocouple sensor were installed at nearest possible to the cylinder head so that the temperature of intake and exhaust ports can be determined to be used inside CFD simulation. The fuel injection supply and ignition timing was controlled intelligently by an electronic control unit (ECU) installed inside the engine. The shape of piston crown employed for the present validation work is the piston A due to the reason that the piston A had been inserted inside the test rig initially.

The comparison was performed in the engine speed of 2000 rpm. The measurement data for intake port temperature and pressure are 302 K and 1.02 bar, respectively. These two data was applied into computational mesh for CFD analysis to represent the real engine modelling. Figure 22 illustrates a comparison between the calculated and experimental pressure curves under the motoring condition during intake and compression stroke. It is indicated that the calculated maximum pressure is in a close agreement with the measured result. Therefore, the CFD computational mesh and calculation performed in this investigation of turbulence characteristics are able to represent the real condition occurred inside the CNG-DI engine and have the capability to be implemented for further intensive calculation. As can be seen, the cylinder pressure obtained from the CFD simulation has the higher value due to the reason that the typical CFD simulations do not take into account the friction losses took place within engine cylinder. Hence, the numerical calculation has the higher cylinder pressure compared to the experimental data and it is usually accepted for any validation of simulation results.

Figure 21: The SCRE test rig of CNG-DI engine

The actual validation of the numerical prediction from CFD results in an internal combustion engine is through the utilisation of some high-cost visualisation equipment, such as particle image velocimetry (PIV), laser Doppler anemometry (LDA) or any visualisation method. In this paper, the limitation of high investment on those equipments has become an obstacle to employ it to validate the CFD data. Therefore, besides the in-cylinder pressure comparison during motoring condition, the other technique of numerical assessment used to validate the results obtained from CFD calculation in this paper is the typical swirl and tumble ratio produced from the other researchers. Theoretically, the magnitude of fluid flow and turbulence parameters are depend on the engine size, speed, valve opening and closing timing, bore and stroke, piston crown, initial pressure and temperature and other engine configuration. For swirl and tumble ratio, the magnitude obtained in this paper are in the range of typical value of swirl and tumble ratio based on the current

literature review [17, 22, 23, 24, 25, 26, 27]. On the other hand, the acquired turbulence parameters in the form of turbulence intensity and length scale also represent the common magnitude for these two parameters from the published literature [23, 24, 26, 27, 28]. Therefore, the investigation on the effect of piston crown to the dynamic flow and turbulence in this paper, which results some parameters mentioned above have adequate comparison to be recognised as a valid CFD result.

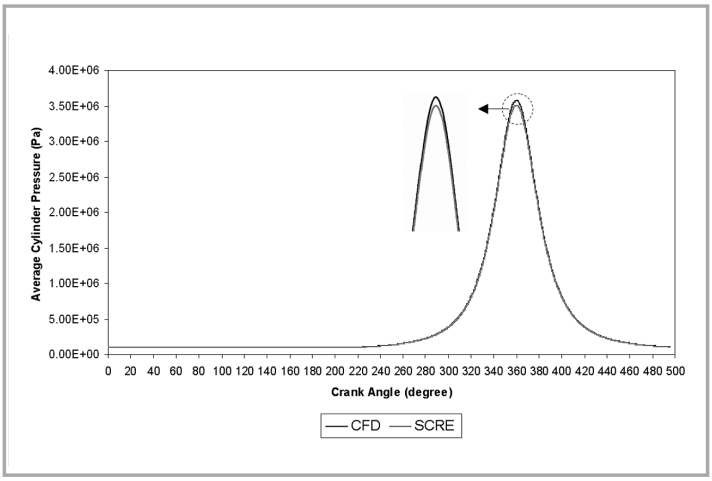

Figure 22: Comparison of calculated and measured in-cylinder pressure under motoring condition

8. CONCLUSION

The investigation and analysis for the characteristics of in-cylinder air motion under motoring condition is numerically carried out by solving the intake and compression stroke by CFD code with the moving mesh and boundary capability. Transient moving valves were exactly modelled to resolve intake-generated swirl and tumble motion as well as the turbulence field characteristics in the area of valve curtain and engine cylinder. The evaluation in present study is carried out for two shapes of piston crown to evaluate the effect of different combustion chamber shape to the fluid flow field and turbulence field for the preparation of air-fuel mixture. The solved calculation of CFD analysis for every crank angle throughout intake and compression stroke is presented to examine and verify the behaviour of those mentioned characteristics for overall piston crowns furnished with its discussions thoroughly. During the intake stroke the shape of the piston crown does play a significant role to the developed large scale fluid motion as the most significant component of mixing parameters during the whole process of engine by characterising it with the swirl ratio, sideways and normal tumble ratio. The small scale motion represented its turbulence field has been calculated by specifying it in the terms of turbulence intensity, turbulence length scale and its kinematic viscosity.

In general, this study shows that in-cylinder CFD predictions yield a reasonable result that allows improving the knowledge of the in-cylinder flow pattern and characteristics during the intake and compression strokes instead of using the experimental test by particle image velocimetry (PIV) or laser Doppler anemometry (LDA). At this moment, this CFD in-cylinder analysis result has not been validated with the experimental result due to the highly experimental equipments, devices and measurement tools. However, the cylinder pressure of motoring condition has been validated against the experimental measurement and it reveals that the developed engine model and its moving mesh have a capability to approach the real engine condition. In addition, the study and analysis presented here represents a first step towards our understanding of air motion field inside cylinder for a CNG-DI engine. Besides of that, CFD can be used as an efficient design tool to develop the other internal combustion engine analysis to produce an optimum engine configuration. For future work, the application of large eddy simulation (LES) model to investigate the behaviour of fluid flow and turbulence field in an internal combustion engine can be performed for better understanding of these complex phenomena of fluid dynamic. However, the relatively high computation cost will be occurred as a consequence from the use of LES model due to their numerical algorithm. Lastly, the optimum piston crown investigated from the present study will be used as a further examination by carrying out it into the combustion and emission formation analysis.

ACKNOWLEDGMENTS

The authors would like to thank the Ministry of Science, Technology and Innovation of Malaysia for sponsoring this work under project IRPA 03-02-02-0057-PR0030/10-04. ■

REFERENCES

[1] Gosman A.D., Tsui Y.Y., and Watkins A.P. (1984). "Calculation of Three Dimensional Air Motion Model Engines." SAE Paper 840229.

[2] Kondoh T., Fukumoto A., Ohsawa K., and Ohkubo Y. (1986). "An assessment of a multi-dimensional numerical method to predict the flow in internal combustion engines." SAE Paper 850500.

[3] Zur Loye A.O., Siebers D.L., Mckinley T.L., Ng H.K., and Primus R.J. (1989). "Cycle-resolved LDV measurements in a motored Diesel engine and comparison with k-ε model predictions." SAE Paper 890618.

[4] Kono S., Terashita T., and Kudo H. (1999). "Study of the swirl effects on spray formation in DI engines by 3D numerical calculations." SAE Paper 910264.

[5] Wakisaka T., Shimamoto Y., and Issihiki Y. (1986). "Three-dimensional numerical analysis of in-cylinder flows in reciprocating engines." SAE Paper 860464.

[6] Brandstätter W., Johns R.J.R., and Wigley G. (1985). "The effect of engine speed on the TDC flow field in a motored reciprocating engine." SAE Paper 850499.

[7] Schapertons H., and Thiele F. (1986). "Three dimensional computations for flow fields in DI piston bowls." SAE Paper 860463.

[8] Theodorakakos A., and Bergeles G. (1993). "Predictions of the in-cylinder fluid motion of a motored internal combustion engine." Entropie No. 174/175.

[9] Henriot S., Le Coz J.F., Pinchon P. (1989). "Three dimensional modelling of flow and turbulence in a four-valve spark ignition engine – Comparison with LDV measurements." SAE Paper 890843.

[10] Mao Y., Buffat M., and Jeandel D. (1994). "Simulation of the turbulent flow inside the combustion chamber of a reciprocating engine with a finite element method." Journal of Fluid Engineering, 116.

[11] Arcoumanis C., Begleris P., Gosman A.D., and Whitelaw J.H. (1986). "Measurements and calculations of the flow in a research Diesel engine." SAE Paper 861563.

[12] Aita S., Tabbal A., Munck G., Montmayeur N., Takenaka Y., and Aoyagi Y. (1991). "Numerical simulation of swirling port valve-cylinder flow in Diesel engine." SAE Paper 910263.

[13] Chen A., Veshagh A., and Wallace S. (1998). "Intake flow predictions of a transparent DI Diesel engine." SAE Paper 981020.

[14] Dillies B., Ducamin A., Lebrere L., and Neveu F. (1997). "Direct injection Diesel engine simulation: a combined numerical and experimental approach from aerodynamics to combustion." SAE Paper 970880.

[15] Celik I., Yavuz I., and Smirnov A. (2001). "Large eddy simulations of in-cylinder turbulence for internal combustion engines: a review." International Journal of Engine Research 2(2): pp 119–48.

[16] Hyun G., Oguma M., and Goto S. (2002). "3-D CFD analysis of the mixture formation processes in an LPG DI SI engine for heavy duty vehicles." Proceedings of the 12th International Conference of Multidimensional Engine Modelling User Group Meeting SAE Congress, Detroit, Michigan, USA.

[17] Kim Y.J., Sang H.L., and Nam H.C. (1999). "Effect of air motion on fuel spray characteristics in a gasoline direct injection engine." SAE Technical Paper Series No. 1999-01-0177.

[18] Payri F., Benajes J., Margot X., and Gil A. (2004). "CFD modelling of the in-cylinder flow in direct-injection Diesel engines." Computers and Fluids, Elsevier Press. 33: pp 995-1021.

[19] Kurniawan W.H., Shamsudeen A., and Abdullah S. (2005). "The development of moving mesh for the half-model simulation of a four-stroke automotive engine. Proceedings of National Seminar of Computational and Experimental Mechanics, CEM 2005, Bangi, Malaysia.

[20] Versteeg H.K., and Malalasekera W. (1995). An Introduction to Computational Fluid Dynamics-The Finite Volume Method, Longman Group Ltd, London.

[21] Launder B.E., and Spalding D.B. (1974). "The numerical computation of turbulent flow." Computer Methods in Applied Mechanics and Engineering, Elsevier Press. 3(2): pp. 269-289.

[22] Heywood J.B. (1987). "Fluid motion within the cylinder of internal combustion engine – The 1986 Freeman Scholar Lecture." Journal of Fluids Engineering. 109: pp. 3-35.

[23] Suh E.S., and Rutland C.J. (1999). "Numerical study of fuel/air mixture preparation in a GDI engine." SAE Paper 1999-01-3657.

[24] Han Z.Y., and Reitz R.D. (1997). "Multidimensional modeling of spray atomization and air-fuel mixing in a direct-injection spark-ignition engine." SAE Paper 970884.

[25] Luo M.J., Chen G.H., and Ma Y.H. (2003). "Three-dimensional transient numerical simulation for intake process in the engine intake port-valve-cylinder system." Journal of Zhejiang University SCIENCE, Zhejiang University Press. 4(3): pp.309-316.

[26] Bailly O., Buchou C., Floch A., and Sainsaulieu L. (1999). "Simulation of the intake and compression strokes of a motored 4-valve SI engine with a finite element code." Oil & Gas Science and Technology – Rev. IFP, Éditions Technip. 54(2): pp. 161-168.

[27] Han Z.H., Reitz R.D., Yang J.L., and Anderson R.W. (1997). "Effects of injection timing on air-fuel mixing in a direct-injection spark-ignition engine." SAE Paper 970625.

[28] Han Z., and Reitz R.D. (1995). "Turbulence modeling of internal combustion engines using RNG k-ε models." Combustion Science and Technology, Amsterdam B.V. Publisher. 106: pp. 267-295.